Applied Energy 288 (2021) 116610

Contents lists available at ScienceDirect

Applied Energy

journal homepage: www.elsevier.com/locate/apenergy

Analysis of derating and anti-icing strategies for wind turbines in cold climates

D.B. Stoyanov [a], J.D. Nixon [a,*], H. Sarlak [b]

[a] Faculty of Engineering, Environment and Computing, Coventry University, UK
[b] Fluid Mechanics Section, Department of Wind Energy, Technical University of Denmark, Denmark

HIGHLIGHTS

- A method is provided for comparing wind turbine derating and anti-icing solutions.
- Anti-icing system viability is established based on cost and icing event frequency.
- Derating outperforms anti-icing during extreme icing events below −10 °C.
- Daily energy losses and ice mass accumulation can both be reduced via derating.
- Wind turbines should operate as normal during mild icing conditions below −10 °C.

ARTICLE INFO

Keywords:
Wind energy
Wind power
Icing events
Cold climates
Tip-speed ratio (TSR)
Ice accretion

ABSTRACT

Wind turbines located in cold climates suffer from reduced power generation due to ice accretion. This paper presents a novel method for comparing and evaluating two emerging ice mitigation strategies: tip-speed ratio derating and electrothermal anti-icing. The method used takes into account accumulated ice mass, net energy losses both during and after an icing event, and financial breakeven points; it is demonstrated for the assessment of the NREL 5 MW reference wind turbine during different icing events. Our results show how derating can be preferred over electrothermal anti-icing and how this changes for different wind speeds, icing conditions, ambient temperatures, and system costs. For a 1-hour extreme icing event, it is expected that derating will reduce accumulated ice mass and daily power loss by up to 23% and 37%, respectively. Anti-icing was identified to be the preferred strategy when there were 42 in-cloud icing event occurrences per year, ambient temperatures were above −5 °C, and the system cost was no higher than 2% of the turbine's capital cost. This research demonstrates to wind turbine operators how different strategies can be selected to improve performance during icing conditions.

1. Introduction

Around a quarter of the world's wind turbine capacity is installed in cold climate sites, where either icing occurs on a regular basis or wind turbines operate in low temperatures, outside their designed operational limits [1]. Ice accretion can have a severe impact on power performance, safety and maintenance [2]. Ice-induced energy losses can exceed 20% of the annual energy production depending on geographical location and wind turbine size [3]. Ice may cause structural imbalances, resulting in prolonged and expensive maintenance. Additionally, ice can be a safety risk [4] as pieces of ice weighting up to 6.5 kg have been thrown 600 m from utility-scale wind turbines [5]. Currently, international standards for cold climate wind farms and universal ice mitigation solutions are not available [6], so further research and development to address these challenges have become an urgent requirement for manufacturers and operators [4,7].

Ice mitigation can be achieved by using pneumatic boots, electro-impulsive/expulsive system, microwave systems, black blades, chemical methods or protective coatings [6,8,9]. Black blades were found effective for light icing conditions [9], while ice protection – achieved by applying icephobic or hydrophobic coatings – was found unrealistic, unless combined with heating systems [9,10]. Chemical methods have been found unsuitable due to their negative impact on the environment [9], while pneumatic boots have not been actively implemented for wind turbine applications due to noise, intensive maintenance and

* Corresponding author.
E-mail address: jonathan.nixon@coventry.ac.uk (J.D. Nixon).

https://doi.org/10.1016/j.apenergy.2021.116610
Received 7 May 2020; Received in revised form 22 January 2021; Accepted 3 February 2021
Available online 18 February 2021

Nomenclature

Variables

A	Area (m^2)
A1	Cost to use anti-icings (£)
a	Annuity factor (%)
B1	Financial losses due to icing (£)
c	Aerofoil chord length (m)
c_e	Price of electricity (p/kWh)
Cp	Power coefficient (-)
E	Energy (MWh)
I	Initial investment (£)
i	Section counter (-)
LWC	Liquid water content (kgm^{-3})
M	Mass (kg)
MVD	Median volume diameter (m)
N	Number of icing days (day)
P	Power (W)
P_W	Wind power (W)
q	Heat Flux (kWm^{-2})
R	Radius (m)
r	Blade radius (m)
s	Relative coordinate (m)
s'	Integration limit
T	Temperature (°C)
t	Time (h)
V	Wind speed (ms^{-1})

Greek

ρ	Air density (kgm^{-3})

Subscripts

A, B, C, D	Blade section location
24	24 h
AI	After icing
CAPEX	Capital cost
DI	During icing
EPB	Energy payback
ICE	Property of ice
M	Modified operational strategy
O&M	Operations and maintenance cost
R	Reference operational strategy
S	Operational shutdown
rel	Relative to the blade
req	Required

Acronyms

AIS	Anti-icing system
CC	Cold climate
NREL	National Renewable Energy Laboratory
TSR	Tip-speed ratio

design difficulties [8,11]. Electro-impulsive/expulsive and microwave systems are being actively researched and due to favourable energy efficiency, low cost, automation ease and low frequency interference , they could be a promising option in the near future [6,11].

Recent reports on the available technologies for cold climate wind energy developments show that wind turbine manufacturers are predominantly investigating electrothermal and hot-air ice protections systems [12]. Additionally, Enercon and Lagerway wind turbine manufacturers use preventive shutdown (i.e. operational shutdown) for their wind turbines in cold climates, which accounts for more than 8.1 GW of installed energy generation capacity [12]. Future ice protection technologies most likely will be focused on electrothermal and hot-air systems, as most of the independent ice protection system providers do not offer alternative solutions [12]. Such technologies in combination with low-cost power maximisation techniques, using rotor rotational speed and pitch setting modifications to reduce ice accretion rate and improve post-icing performance, could be the most desirable choice for optimal wind turbine adaption to cold climates. Despite Electrothermal anti-icing [6,13–17] and derating [18–20] being actively researched for ice mitigation, to the authors' knowledge, no method has been developed to compare them and the following research questions remain unknown and need to be answered:

I. can derating improve power performance in comparison to anti-icing solutions for wind turbine ice-mitigation and, if so,
II. under what conditions will derating be the preferred strategy for wind turbine's operating in cold climates?

There are two main types of thermal icing protection systems: protecting the blade surface to prevent ice deposits (anti-icing) and removing deposited ice by minimising its adhesion to the protected surface (de-icing) [9,21]. A significant disadvantage for both technologies is the required power to operate them and a failure of heating elements can lead to structural damage and rotor imbalances. Operating de-icing technology during the rotation of wind turbine rotors could be a safety risk due to the risk of de-iced pieces being thrown, which is most likely the reason why most, but not all, of the already implemented de-icing technologies are reported to require wind turbine stoppage prior to heating for ice removal [12,22,23]. Anti-icing technologies are now emerging as available and efficient options for protecting wind turbine blades [24]. However, only a few reports provide experimental or field data on the performance of anti-icing systems. An electrothermal ice protection system, fitted to a 220 kW wind turbine, installed in Finland, was reported to require 6% of the rated power for operation [3]; for a 600 kW wind turbine in the same region it was 5% [25]. Values between 3.6% and 10.4% were reported for wind farms in Norway [23]. The variation in required heating highlights the importance of well adapted and designed ice protection systems, which was also identified by Roberge et al. [26] and Catting et al. [27], after investigating wind turbine field data.

Further research on anti-icing systems has focused on evaluating electrothermal anti-icing system power requirements during an icing event without accounting for post-icing event losses [13,14,28], which results in under predicted ice-induced losses. Thus, there is a need to investigate the performance of electrothermal anti-icing techniques when considering icing losses both during and after icing events, whilst also accounting for a system's financial viability.

An alternative approach for mitigating ice-induced power losses is to implement an operational strategy that allows for slowing down the rotational speed of a wind turbine (tip-speed-ratio derating) to reduce ice deposition, thereby improving power characteristics after an icing event ends [20]. In [19], it has been shown that improved conversion efficiencies can be obtained at the end of an icing event in comparison to operating a wind turbine according to its reference operational strategy. Homola et al. [29] investigated two operational strategies to control the operational tip-speed-ratio (TSR). They found that over a range of wind speeds the power output can be increased by 10% by modifying the operational TSR. A method to systematically determine the ideal TSR values during an icing event was established by the authors of this paper in [18]; we showed that the lost energy from slowing down a wind turbine can be recovered within 0.5–2.5 h after an icing event ends due to accumulated ice mass being reduced by up to 30%. Both anti-icing

and TSR strategies cause power reduction during active icing events. Therefore, potential annual net energy gains that can be achieved by these different ice-mitigation approaches need to be known for a range of icing events and operational periods.

The aim of this research is to establish a method for comparing and selecting electrothermal anti-icing and tip-speed ratio derating strategies for wind turbines operating in cold climates. This is timely as electrothermal anti-icing systems and derating strategies for wind turbines are now emerging as solutions for ice mitigation; however, research is needed to ensure that they can be effectively implemented to reduce ice accretion and achieve gains in power performance. This research sets out to investigate how the preferred choice of strategy can change based on financial costs and icing condition variations.

Section 2 outlines the research methods, which include icing event, anti-icing and operational strategies modelling. The results and the discussion are provided in Section 3. Section 4 evaluates the current approach and gives suggestions for further work. In Section 5, the main findings and the implications of this work are summarised.

2. Methodology

In this study, it is assumed that two approaches for ice mitigation could be applied to a utility scale wind turbine during an in-cloud icing event: derating scenarios realised by modifying the operational TSR and electrothermal anti-icing. In addition, operational shutdown is considered as it is still being used as an ice protection method by some manufacturers [12]. Even though shutdown leads to prolonged periods of zero power output, it is of interest to quantify its viability against other technologies, as it is an inexpensive and easily realisable method. The NREL 5 MW reference wind turbine is considered for the evaluation of these different ice mitigation techniques.

The performance of the wind turbine for each ice mitigation technique is analysed by modelling the energy yield for a 24-hour period, with an icing event occurring at the start of the analysis period. To model the operation of the NREL 5 MW reference wind turbine during in-cloud icing, the method outlined by the same authors in [18] is used, which utilises LewINT for simulating ice accretion [30], Qblade [31] for aerodynamic and power performance analysis and an energy payback time scheme for comparing derating scenarios realised by modifying the operational TSR. The anti-icing energy requirements are modelled using LewINT, which provides the needed heat flux to keep an aerofoil surface at a prescribed temperature. Two surface temperatures of −5 °C and −15 °C and two variations of the protected aerofoil surface, full protection and water impingement zone protection, are chosen for the anti-icing analysis. The viability of the anti-icing operational approach is estimated by using a return investment cost model [25], which is based on the difference between the energy lost due to ice accumulation and the energy required to operate an anti-icing system. To investigate how the suitability of the operational strategies might change according to the weather conditions, two additional scenarios are modelled, which consider a lower wind speed and a longer mild icing condition.

2.1. Icing conditions and ice mass calculation

A 1-hour in-cloud icing event and a wind speed of 10 ms^{-1} is initially considered, with a liquid water content (LWC) of 5×10^{-4} kgm^{-3} and droplet median volume diameter (MVD) of 25×10^{-6} m. The icing event is based on environmental parameters typical for relatively short icing events [18] Although icing conditions vary with location and in time, energy yield losses and operational strategy performance are often studied by using fixed operational and meteorological conditions, as seen in [19,29,32]. The relative speed to the outermost blade section for this event was calculated to be 71.4 ms^{-1} for a reference TSR of 7.5 (TSR_R), and its water collection efficiency was modelled with LewINT to be 0.4 on average. The ice accumulation rate for the selected conditions was calculated to be approximately 0.053 m/hour, which can be classified as an extreme icing event according to an icing severity scale proposed by Lamraoui, Fortin, Benoit, Perron and Masson [33]. As anti-icing power requirements and ice shapes vary with ambient conditions, a range of ambient temperatures (T_{AMB}) from −30 °C to −5 °C were studied for this icing event. Two additional icing scenarios were modelled to investigate how the wind turbine performance would vary if operational and weather conditions change. The first additional scenario includes lowering the wind speed to 7 ms^{-1} and keeping the weather conditions unchanged. In the second scenario, the icing duration was increased to 4 h and the LWC and MVD were changed to 3.5×10^{-4} kgm^{-3} and 20×10^{-6} m, respectively, representing milder conditions. Thus, three icing events (see Table 1) are defined with a wind speed variation and a duration reflecting real cold climate conditions from northern Europe. Two years of field data specified the icing duration frequency to be between 1 h and 4 h [28]. In addition, the European wind atlas [29,30] shows that the expected wind speeds for cold climate sites in Europe are between 7 ms^{-1} and 10 ms^{-1}.

Although the icing conditions (i.e. LWC, MVD, T_{AMB}, V) are not completely independent, the LWC, MVD and V were fixed for the defined icing events. T_{AMB} was varied to study how this would change the viability of an anti-icing solution. Such assumptions are often made in research studies, which consider a range of icing events [18,34–36]

The power output of the wind turbine was modelled using strip theory approach, which is widely used for modelling the performance of wind turbines in icing conditions [19,29]. Ice accretion only on the outer half of the blade was modelled, as previous research has shown that it is the most sensitive area to icing. This approach provides a good representation of an iced wind turbine blade and reduces the computational intensity required for further modelling [19,29,32]. The power output during icing conditions was calculated by modelling the expected 2D ice shapes at four main sections, as depicted in Fig. 1. Each ice shape was modelled accounting for the complex thermodynamic equilibrium on the surface of the blade during icing and its dependence on the environmental parameters [30].

The ice mass was modelled at different TSR settings. Instead of using the mass of water which freezes on impact with the aerofoil surface, as reported in [18] and also used in [32,36], the total ice mass ($M_{ICE,T}$) was modelled in this study. The total ice mass, $M_{ICE,T}$, is calculated as shown by Eq. (1), where $A_{ICE,i}$ is the area of the ice shape at each blade section, ΔR_i is the blade section width, ρ_{ICE} is the density of the ice and i is the blade section counter. The assumptions made during the modelling of the ice mass include constant ice density of 917 kgm^{-3} and symmetrical ice deposition on the rotor blades, as in previous studies [32,36]. It should be noted that this assumption might produce higher ice mass estimations for lower $T_{AMB,}$ when the density of the ice is typically lower. However, for ambient temperatures between −10 °C and 0 °C, the results would not be affected significantly due to the formation of denser ice types at these temperatures [37].

$$M_{ICE,T} = (A_{ICE,A}\Delta R_A + A_{ICE,B}\Delta R_B + A_{ICE,C}\Delta R_C + A_{ICE,D}\Delta R_D)\rho_{ICE} \quad (1)$$

Table 1
Definition of icing events A, B and C, at different wind speeds (V), and temperatures(T).

Event	LWC (10^{-} kg m^{-3})	MVD (μm)	Duration (hour)	V (m s^{-1})	T_{AMB} (°C)
A	5	25	1	10	−30 to −5
B	5	25	1	7	−30 to −5
C	3.5	20	4	10	−30 to −5

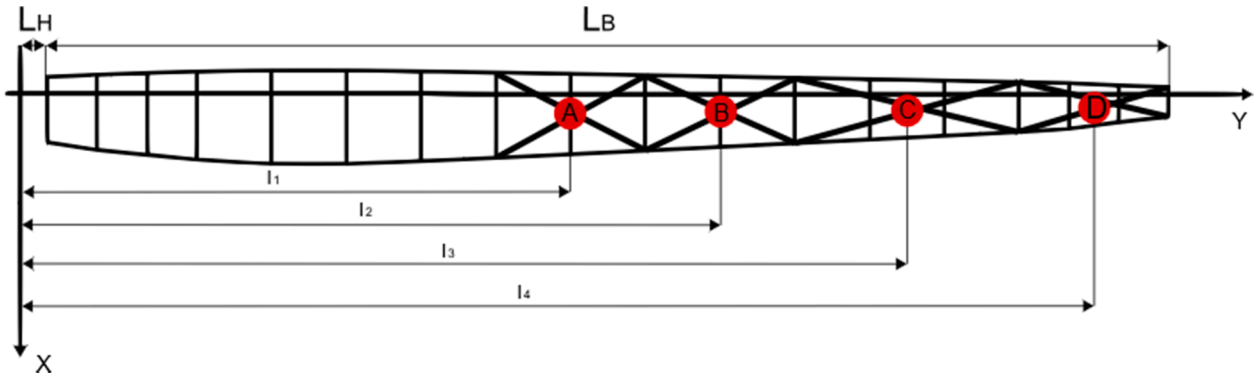

Fig. 1. NREL 5 MW wind turbine blade sections A, B, C and D used for the estimation of $M_{ICE,T}$ and the ice shapes with respective distances to the rotor's hub centre -l1, l2, l3 and l4, which are at 52%, 65%, 80% and 94% of the blade's radius [18]; for sections A, B, C and D the spans are respectively 8.2 m, 8.2 m, 12.3 m and 8.2 m, and the mid-section chord lengths are 3.7 m, 3.22 m, 2.65 m and 1.94 m.

2.2. Anti-icing power estimation

One-dimensional anti-icing analyses using LewINT® ice accretion software have been reported to provide satisfactory results for heat flux estimations [30,38]. The composition of the blade sections and the material thermal properties are as pre-defined in LewINT® [14]. It is assumed that the anti-icing will be operated in a running-wet state. This ensures that the impinged water on the surface of the aerofoil will be in liquid phase rather than being evaporated upon impact [30]. The target surface temperature (T_{SURF}) was chosen to be either 5 °C or 15 °C, as these surface temperatures are typically considered for an anti-icing system (AIS) design [28,39].

To investigate how the protected area affects the power demand for the chosen icing conditions, two simplified protected surface areas are considered, as shown on Fig. 2a-b. AIS Area 1 covers the whole area of the aerofoil blade section (Fig. 2a). AIS Area 2 protects only the water freezing zone (Fig. 2b), which is modelled in LewINT®, accounting for the operational and icing parameters. Even though full protection of the surface would require the highest possible power requirement, it indicates the upper limit of needed power, which can be used to establish the maximum energy required for an AIS. The impingement area protection would require the least power, as normally the water impingement zone is narrower than the ice formation zone on the aerofoil surface [28,40,41]. However, it can be used to establish lower idealised limits of the needed power for operating an AIS. When impingement area anti-icing is chosen, resultant ice shapes are expected if the supplied heat flux to the surface of the blade is insufficient to keep the impinged water in a liquid phase [42]. For this study, a conservative assumption is made that no residual ice shapes will form, as this would require an AIS system design layout to be modelled and sized.

The required power, P_{Req}, to run an AIS is calculated by integrating the elemental heat flux, q_i, along the aerofoil surface (Fig. 3) and the blade section width, ΔR_i (see Eq. (2)). The needed heat flux for each blade section is estimated by modelling q_i at the mid-section (i.e. locations A, B, C and D in Fig. 1), where the 2D ice formation simulations have been performed. $P_{Req.}$ for anti-icing is approximated by assuming constant distribution of q_i along ΔR_i, which has been shown to increase linearly along relatively short blade sections and with wind speed [15,43]. The protected area type (Fig. 2a-b) defines the limits of integration and the needed power. Fig. 3 shows an example distribution of the needed heat flux along the unwrapped distance, s, (i.e. the coordinate system fixed to the blade surface), normalised by the blade section chord length, c. Thus, for different protected areas the limits of integration would differ and can be defined as $-/+s'$, which in the case of full area protection (Fig. 2a) become -/+ s/c. Additionally, depending on the location of the blade section, the heat distribution needed for maintaining the desired surface temperature would change, although the peak would always be near the stagnation region.

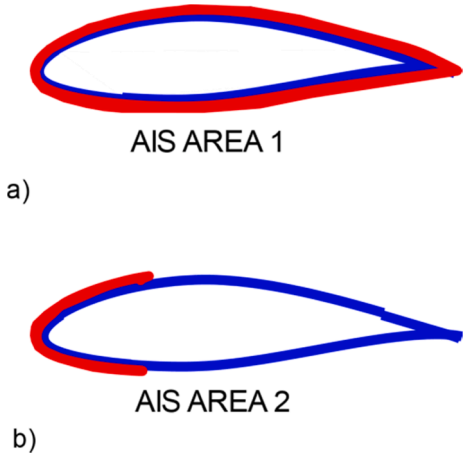

Fig. 2. a-b AIS for full surface (a) and impingement zone (b) protection. The required power to operate AIS is calculated at the mid-section of the modelled blade sections A, B, C and D.

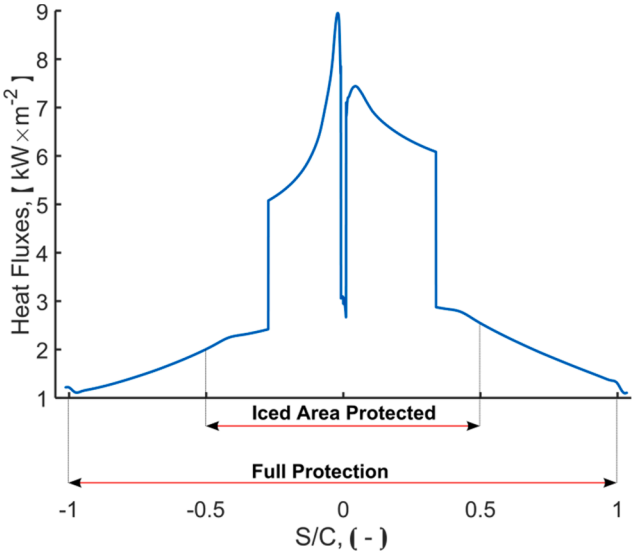

Fig. 3. . An example integration limit for different protection areas to estimate the amount of required power needed for anti-icing.

$$P_{Req.} = \Delta R_i \int_{-s'}^{s'} q_i ds \quad (2)$$

2.3. Evaluation of ice mitigation strategies

Operating according to different operational strategies results in variable wind turbine performance. Fig. 4 shows how the instantaneous power output of a 5 MW wind turbine varies for different strategies during a 1-hour icing event at the start of a 24-hour period. For this study, there are four types of sustained power losses: losses due to operation according to the reference tip-speed ratio (TSR_R) strategy; losses from intentional power drop from derating (TSR_M) and ice accumulation; net power loss from running AIS; and no power output during complete shutdown (standstill).

The net power drops due to AIS operation – and the subsequent daily net energy loss – is limited by the duration of the icing event, as the blade surface should be clean once the icing event ends and assuming that there are no ice residues. The assumption is made that for anti-icing the blade would be clean at the end of the icing event and net power output would be restored to the reference TSR ($TSR_{R,clean}$). It should be noted that in reality ice residue is possible even with an ice protection system due to uneven heating and heating element layout design. Thus, additional losses can be incurred, which can affect the evaluation of ice mitigation strategies.

Operating without an AIS leads to ice accumulation. Instantaneous power output is therefore decreased for the reference strategy and derating both during ($TSR_{DI,R}$ and $TSR_{DI,M}$) and after ($TSR_{AI,R}$ and $TSR_{AI,M}$) an icing event. Fig. 4 represents how deliberately slowing down the TSR to reduce ice build-up could result in a higher energy yield over a given reference period than the reference operation, once an icing event ends. As natural mechanisms of ice removal (melting, shedding and wind erosion) are not modelled in this study, lower and upper limits for the expected power losses were considered. The lower limit assumes that all ice formation is removed immediately after the end of the active icing event (i.e. the power output at the end of the event recovers to the clean rotor state, $TSR_{R,\ Clean}$). The upper limit is defined considering no ice shape changes after the icing event for the next 23 h, which leads to constant reduced power after the active icing event, providing the wind speed remains unchanged. The actual performance post icing will depend on the rate of the ice removal for steady state analysis.

Operational shutdown is modelled as instantaneous power output recovery after the icing event, with no power output during the icing event. However, in reality, melting time of up to 6 h have been reported for wind turbines using operational shutdown [44]. Long recovery times lead to extreme energy losses (e.g. 2 h of stoppage for a 5 MW wind turbine results in an 8.3% daily energy loss). Therefore, operational shutdown only during the event and instantaneous power recovery post-icing event is an idealised scenario and it indicates if shutdown can become a viable solution in comparison to other operational strategies. operational shutdown is viable during this idealised case, a maximum viable stoppage time for melting would be established. Total energy loss (E_{Loss}) estimations for the 24-hour period have been calculated for each strategy in relation to the energy that could have been achieved for non-icing conditions (E_{CLEAN}), *Eq. (3)*, with E_{AIS}, $E_{TSR,M}$, $E_{TSR,R}$ and E_S representing the daily energy generated for the different potential modes of operation. The subscripts denote operation with anti-icing (AIS), derating via a modified tip-speed ratio (TSR,M), a reference tip-speed-ratio (TSR,R) and operation shutdown (S), respectively.

$$E_{Loss} = \left|E_{CLEAN} - E_{AIS/TSR,M/TSR,R/S}\right| / E_{CLEAN} \quad (3)$$

A break-even scheme, outlined in [25,45], is used to determine when an AIS operational strategy is a viable solution for ice mitigation. The scheme is based on the price of electricity, c_e, the yearly investment for implementing the system I, Eq. (4), an annuity factor, a, and the difference in lost energy from ice deposition and net energy reduction due to operating AIS ($E_{LOSS} - E_{REQ}$). The estimation is performed by limiting the cost of operation *A1, Eq. (5)*, to be less or equal to the loss from icing *B1, Eq. (6)*. When solving Eq. (5) and Eq. (6) simultaneously for the number of icing days, N, for an AIS to break-even in a year, Eq. (7) is obtained. The calculations are performed considering an initial investment cost of £ 3.9 M for the reference wind turbine [46,47], electricity price of 5p/kWh [46], annuity factor of 12.5 [48] and annual operations and maintenance expenditure, $AIS_{O\&M}$, of 2% from the initial investment for the anti-icing system [25]. The initial cost of an anti-icing system, AIS_{CAPEX}, can be up to 5% of the wind turbine capital cost [21] and in this study a range from 2 to 5% is investigated.

$$I = \frac{\overline{AIS_{CAPEX}}}{a} + AIS_{O\&M} AIS_{CAPEX} \quad (4)$$

$$A1 = I + c_e E_{REQ} N \quad (5)$$

$$B1 = c_e E_{LOSS} N \quad (6)$$

$$N \leq I / (E_{LOSS} - E_{REQ}) c_e \quad (7)$$

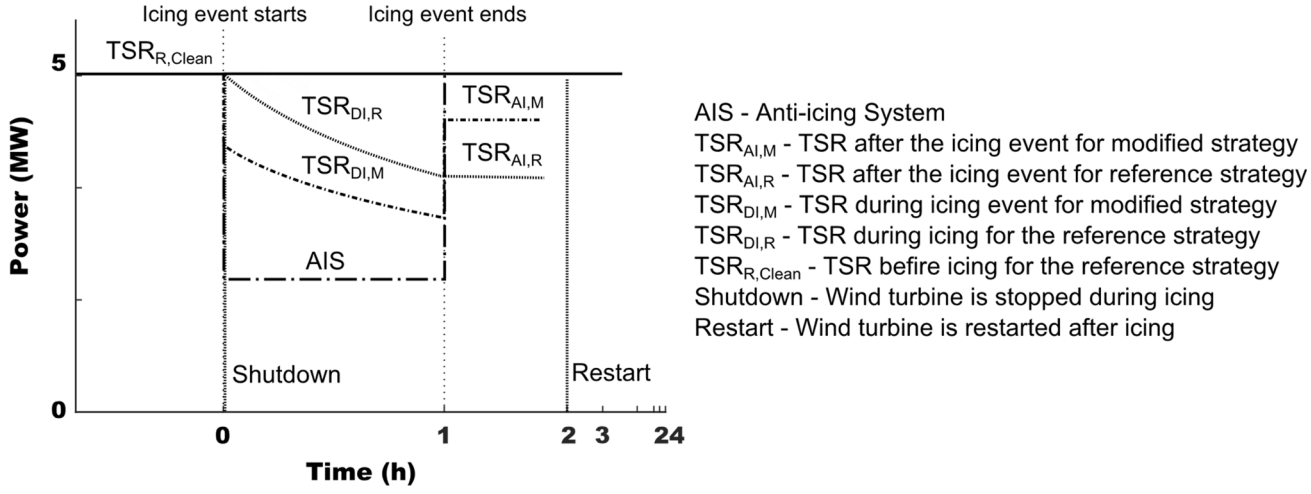

Fig. 4. . Instantaneous power output for a 5 MW wind turbine before, during and after a 1-hour icing event for different operational strategies in a 24-hour operational period.

3. Results and discussion

3.1. Comparison and evaluation of anti-icing and derating for icing event A

In this section, the ideal derating scenario (TSR_M) for the defined icing event in 2.1 is initially established using the energy payback time method as detailed in [18]. By considering the daily net energy losses, an AIS strategy is compared with the selected derating scenario, reference TSR and shutdown strategies.

To identify the most suitable TSR_M for the defined icing conditions in 2.1, energy payback times and ice mass accumulation were modelled. The operational TSR during icing (TSR_{DI}) was chosen to achieve the shortest energy payback time (t_{EPB}). The minimum operational TSR for the NREL 5 MW wind turbine, at a wind speed of 10 ms^{-1}, is 5 [18]; this is based on the original definition of the wind turbine and the chosen electrical generator [49]. Thus, t_{EPB} was calculated considering a TSR range between 5 and 7.5.

Energy payback time estimations for the extreme icing event are shown in Fig. 5a-d. The results indicate that for most of the cases either a TSR_{DI} of 6.5 or 7 should be chosen, as they provided the shortest energy payback time. The energy payback time for a TSR_{DI} of 6.5 was predicted to be more than double in comparison to a TSR_{DI} of 7. However, the latter was not found to be a possible option for operation at T_{AMB} of −5 °C. Thus, a TSR_{DI} of 6.5 was chosen as it outperformed the TSR_{DI} of 5 for T_{AMB} of −30, −20 and −5 °C, while for T_{AMB} of −10 °C the difference in the resultant t_{EPB} was less than 1 h (Fig. 5c). The expected energy payback time for operating the wind turbine at a TSR_{DI} of 6.5 and a TSR_{AI} of 7.5 was estimated to be 6.3, 4.8, 4.6 and 1.9 h for T_{AMB} of −30, −20, −10 and −5 °C, respectively.

When selecting derating, both ice mass reduction and energy payback time should be considered. Fig. 6 depicts how the accumulated ice on the wind turbine rotor varies with TSR_{DI}. Operating at a TSR_{DI} of 5 resulted in the slowest rotational speed of the rotor, which led to the lowest ice deposition rate and the least accumulated ice mass over the range of ambient temperatures. When TSR_{DI} was increased to 6.5, the total ice mass on the rotor increased to around 63–78 kg: roughly

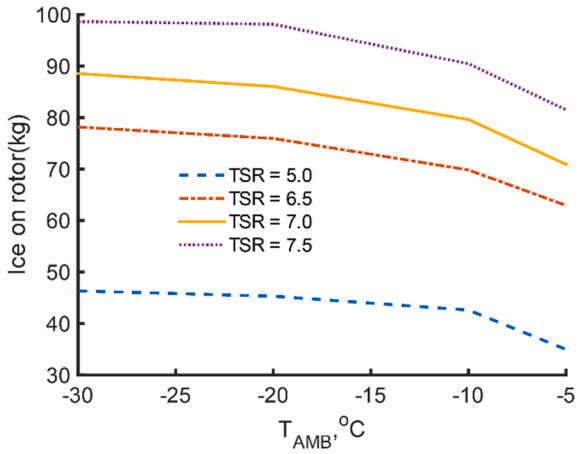

Fig. 6. Ice mass accumulation on the wind turbine rotor during an extreme icing event and its variation for a TSR_{DI} 5 to 7.5 (b).

70–80% more ice. Operating at a TSR_{DI} of 6.5 led to approximately 23% less ice mass in comparison to a TSR_{DI} of 7.5 (TSR_R). Based on the t_{EPB} and ice mass results, a TSR_{DI} of 6.5 and a TSR_{AI} of 7.5 have been chosen as the most suitable TSR_M option for comparison with other ice mitigation strategies.

The performance of the wind turbine was analysed by modelling the daily net energy losses (E_{24}) for every operational strategy. Each strategy would lead to different power losses, as described in Section 2.3. Fig. 7 depicts how these losses vary over the range of considered temperatures for the alternative operational strategies. For the reference operational strategy and derating (i.e. TSR_R and TSR_M, respectively), the daily net energy reduction is shown as an area with lower and upper limits. The lower limit corresponds to the idealised case with deposited ice removed immediately after icing, while the upper limit shows the incurred losses if ice stayed during the 23 h of operation after the 1-hour icing event. The operational strategy that ensures the lowest E_{24} is an indication of the best approach for operation during icing conditions.

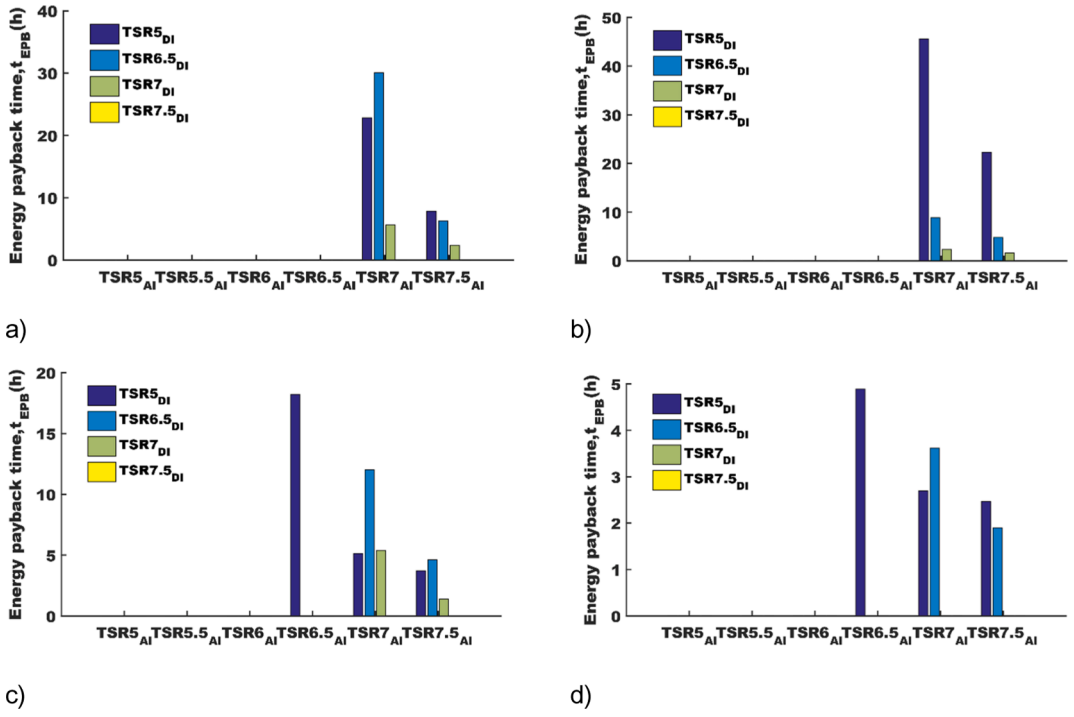

Fig. 5. a-d: Energy payback time (t_{EPB}) for ambient temperatures (T_{AMB}) of −30 °C (a), −20 °C (b), −10 °C (c) and −5 °C (d).

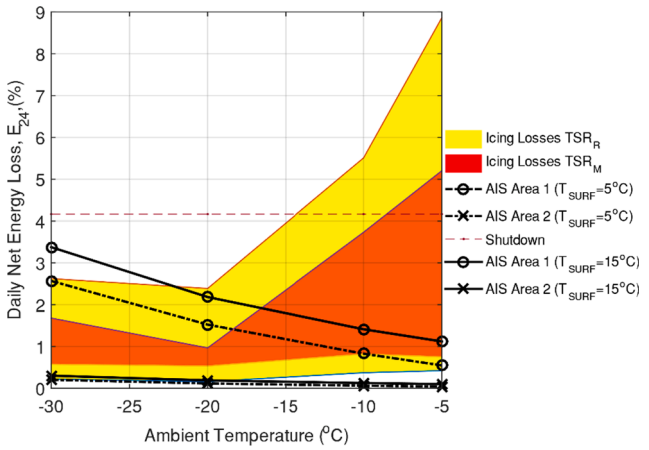

Fig. 7. Performance graph indicating the variation in net daily energy loss for ambient temperatures ranging from −30 °C to −5 °C when derating, AIS and shutdown ice mitigation strategies are utilised (minimum and maximum daily net energy losses for TSR_R are denoted by a green and a red line).

The reference operational strategy and derating allow for ice to form on the blades, leading to deteriorated performance. Fig. 7 shows that between 0.2 and 8.7% less energy would be generated if the wind turbine's reference operational strategy, TSR_R (i.e. is 7.5), was followed. However, when operated at TSR_M (i.e. TSR_{DI} of 6.5 and TSR_{AI} of 7.5), the maximum incurred losses reduced to 5.2%, which is a 37% decrease. The highest energy reduction was found at T_{AMB} of −5 °C, as typically more abrupt ice shapes form in such conditions. In comparison to TSR_R, the overall improvement in the wind turbine performance for the TSR_M is identifiable by the smaller area depicting E_{24}.

Fig. 7 shows when anti-icing will be the preferred operational strategy to minimise daily net energy losses. Considering an average of E_{24}, based on the upper and lower limits for derating and the reference strategy, AIS Area 1, at a surface temperature of 15 °C, would be the preferred strategy for ambient temperatures above −10 °C. This would change to −15 °C, if T_{SURF} was 5 °C. The energy to operate the AIS Area 1 strategy is higher for lower T_{AMB} because the increased convective cooling needs to be balanced from the supplied heat flux. It is interesting to note that for T_{AMB} lower than −15 °C, the TSR_M was estimated to provide the best ice mitigation effect, which infers that derating for some icing conditions can be a more effective ice mitigation technique than AIS based on entire blade surface heating.

Water impingement zone protection (AIS Area 2) would ensure the lowest E_{24}. However, this result corresponds to the minimum E_{24} that would be sustained when AIS is used, as the water impingement area is generally smaller than the ice build-up area, especially in glaze icing conditions (i.e. T_{AMB} higher than −10 °C and high LWC and MVD values). The margins in predicted daily net energy losses between the other strategies and AIS Area 2 can be used for optimisation purposes of AIS Area 2, which might include wider protection area and higher T_{SURF}. Fig. 7 highlights how the importance of having a well-designed AIS protection area increases at lower ambient temperatures.

The operational shutdown strategy led to constant daily net energy losses of approximately 4%. The results show that complete shutdown might be preferred for temperatures between −10 and −5 °C, if ice was to remain on the turbine blades for more than 23 h after the active icing event and it was not possible to implement TSR_M and/or AIS strategies. These results were obtained with the assumption that the recovery time to ice-free blades for this operational strategy is 1-hour. However, in reality, ice might need more time to melt or could accrete during the shutdown, if the wind turbine is set to idle conditions. It is concluded that operational shutdown is not a viable solution for ice-induced energy loss mitigation.

The number of average icing days for AIS Area 1 and AIS Area 2 to reach a break-even point in comparison to the other strategies is shown in Fig. 8a-b. This was modelled by comparing the differences in the expected daily net energy losses. The break-even period for incorporating AIS was obtained using the scheme outlined in Section 2.3 and the average of the E_{24} for both TSR_R and TSR_M (see Fig. 7). The calculations were made by choosing AIS_{CAPEX} to be 3.5%, while error bars indicate how the break-even period would change if the cost of the system was as low as 2%, or as high as 5% of the wind turbine's capital cost. For ambient temperatures above −5 °C and T_{SURF} of 5 °C, AIS Area 1 would be preferred to TSR_R, if there were between 42 and 104 days of extreme icing. In comparison to a TSR_M and shutdown, this increased to 70–175 and 47–118, respectively. The number of icing days per year to reach viability decreased by 11, 17 and 12%, when AIS Area 2 was compared to TSR_R, TSR_M and shutdown, respectively. However, in comparison to other operational strategies, at least 77 days of extreme icing would be required for AIS Area 2 to be preferable at ambient temperatures above −10 °C. When the surface protection was changed to 15 °C, for the same T_{AMB}, the needed icing days for AIS Area 1 increased by 16% to 31%. For lower ambient temperatures, the results highlight the importance of having an optimised anti-icing system from both a cost and performance perspective, as the potential range in number of icing days required per

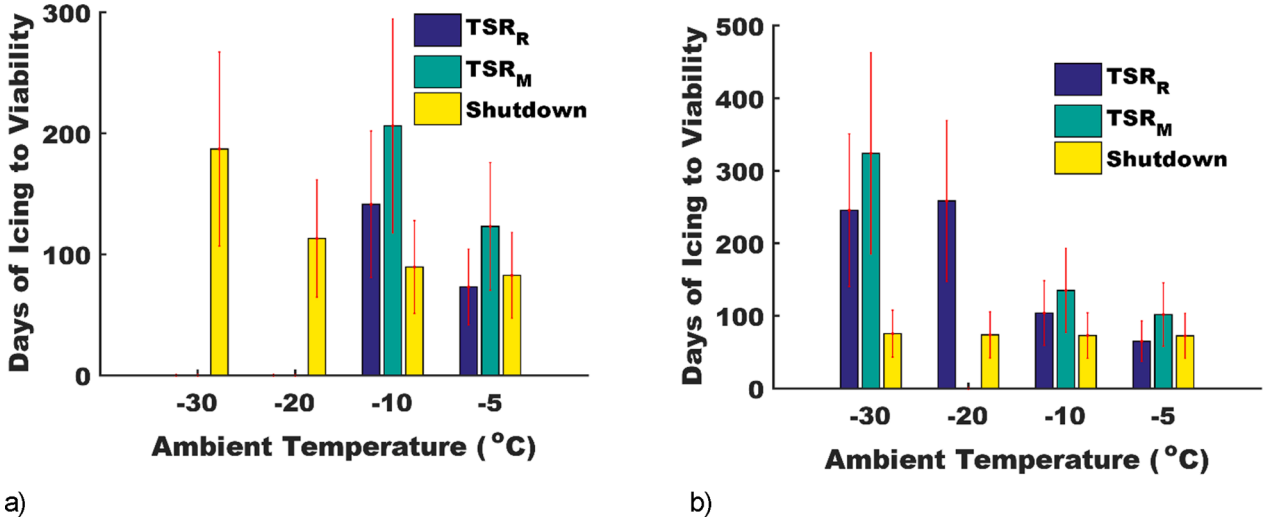

Fig. 8. a-b: Number of icing days per year, which are required for the AIS Area 1 (a) and AIS Area 2 (b), at surface temperatures of 5 °C, to be a viable solution, given the expected daily energy losses for other ice mitigation operational strategies.

year for viability is significant. Nevertheless, in Scandinavia, central Europe and the Apennines, icing events frequency can be more than 30 days per year [3].

3.2. Variation in wind speed and meteorological conditions – Icing events B and C

At a wind speed of 7 ms^{-1}, it was found that derating could not provide improved performance, as it led to higher or comparable energy losses, which is identifiable from the overlapping of E_{24} regions for TSR_M and TSR_R on Fig. 9a. Thus, the TSR_M analysis showed how it is better to operate the wind turbine following TSR_R or using an alternative operational strategy. The results suggest that operating at TSR_R was preferable because, for T_{AMB} between −30 and −15 °C, the daily energy losses would be no higher than 1% and the additional ice mass would be only 54 kg (Fig. 9b), which is small in comparison to the weight of the blades (i.e. approx. 110 tons). Because of the relatively small daily energy losses (less than 10%), anti-icing would not be a viable option for these operational conditions as shown in Fig. 10a-b.

For a long event with smaller LWC and MVD values, higher daily energy losses could be expected as shown on Fig. 9c. The TSR_M strategy was found effective for T_{AMB} between −10 and −5 °C, with higher losses predicted for TSR_R. For a TSR_{DI} of 7 and a TSR_{AI} of 7.5, the estimated payback time would range between 0.8 and 14.5 h and the ice accumulation mass would reduce by around 11% (see Fig. 9d). However, TSR_R should be considered for temperatures lower than −10 °C (Fig. 9c).

Fig. 11a-b shows that if AIS Area 1 cost could be brought down to 2% of the wind turbine capital investment, the system would be viable for ambient temperatures above −5 °C and a T_{SURF} of 5°. In comparison, the icing days to reach viability for AIS Area 2 reduced by 22, 42 and 10% against TSR_R, TSR_M and shutdown, respectively. The main difference for the results was the amount of maximum sustained daily energy losses (16%), which is high because of the prolonged icing event duration.

To summarise, we found that:

- For 1-hour extreme icing events with wind speeds of 10 ms^{-1} and ambient temperatures below −10 °C, derating outperformed anti-icing solutions by reducing energy losses up to 23%
- For a wind speed of 7 ms^{-1} and long, mild icing conditions, at temperatures below −10 °C, the preferred option was to maintain the wind turbine's reference operational strategy.
- Anti-icing was the preferable ice-mitigation strategy for ambient temperatures above −5 °C during both short extreme and long mild conditions, provided the cost of the anti-icing system can be kept low and there were a significant number of icing days so that financial viability could be achieved.

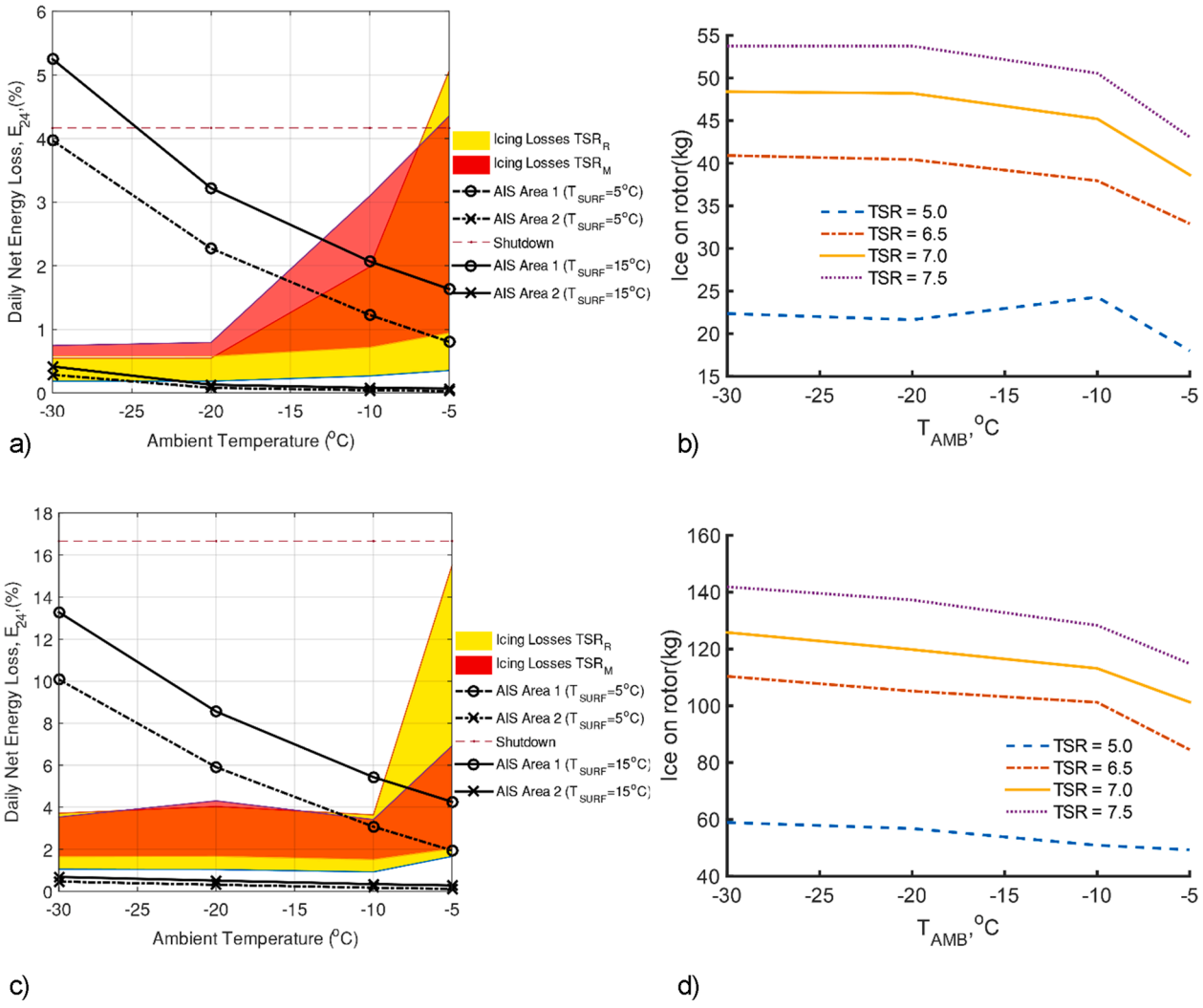

Fig. 9. a-d: Daily energy loss (a and c) and total ice mass (b and d) for a 1-hour long icing event at a wind speed of 7 ms^{-1} (a-b) and a milder 4-hour long icing event at a wind speed of 10 ms^{-1} (c-d).

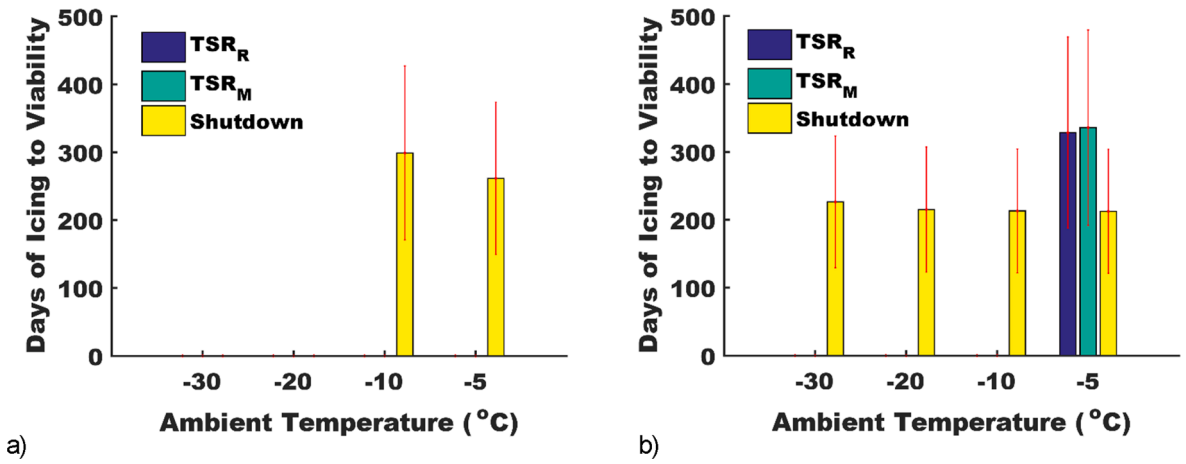

Fig. 10. a-b: Number of icing days per year, which are required for the AIS Area 1 (a) and AIS Area 2 (b), at a surface temperature of 5 °C, to be a viable solution, given the expected daily energy losses for other operational strategies; the wind speed is 7 ms^{-1} and the duration of the icing event is 1 h.

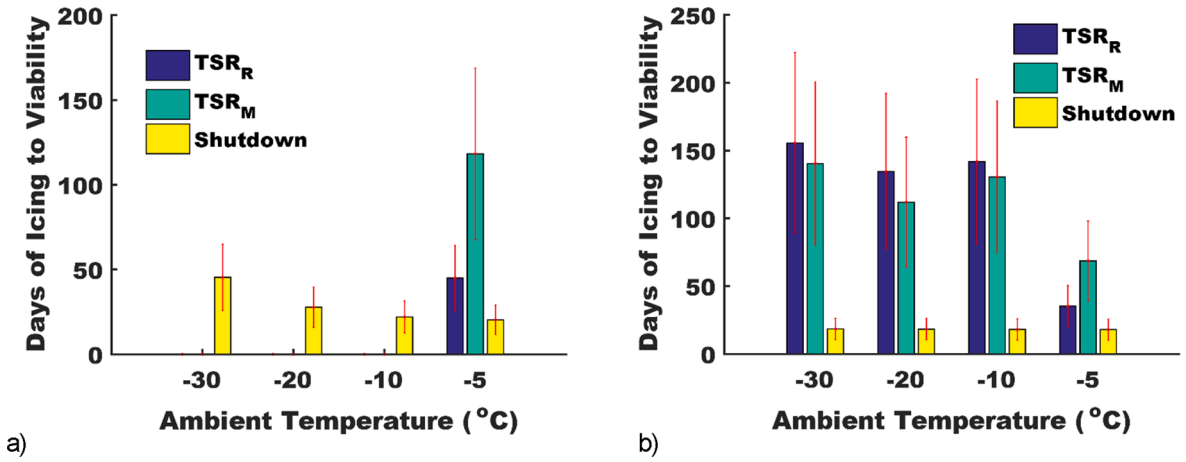

Fig. 11. a-b: Number of icing days per year, which are required for the AIS Area 1 (a) and AIS Area 2 (b), at a surface temperature of 5 °C, to be a viable solution, given the expected daily energy losses for the other operational strategies; the wind speed is 10 ms^{-1} and the duration of the icing event is 4 h.

3.3. Sensitivity of results

The sensitivity of the results based on anti-icing system cost and potential post-icing losses has been highlighted. However, the results are also sensitive to the method used for determining ice-induced power losses, which depending on the aerodynamic analysis tool can introduce varying levels of uncertainty [50,51]. As XFoil is used in this study, the accuracy of the simulations is expected to be reduced when large separation regions form due to highly protruded shapes [18]. The shapes for event A after 0.25, 0.5 and 1 h of icing in Fig. 12a-c illustrate how the contour of section D would change. In Fig. 13 the aerodynamic degradation for these shapes was obtained by using experiments and XFoil simulations. The lift characteristics of the final shape (see Fig. 13c) were measured using a three component balance fitted in an AF100 sub-sonic wind tunnel [52]; the test article was a 3D printed NACA 64–618 aerofoil with a chord length of 0.125 m and a span of 0.303 m. The maximum achievable Re was 160 000, which imposed limitation for achieving good dynamic similarity with actual operating conditions. The degradation of the lift characteristics, at an angle of attack of 4.5°, was calculated to be 25% in XFoil, while the experimental value of 3.9% was obtained. For AoA between 6° to 12° the degradation ranged from 6%-18% and 15%-24% for XFoil and the experimental values, respectively. Hudecz [50] provided experimental data for a similar icing event and the same aerofoil, using an icing research tunnel; the degradation of the lift was found to be around 23% to 36% for AoAs ranging from 4° to 11°. Numerical results obtained using Fluent for slightly different icing parameters on the same aerofoil showed around a 15% lower lift force at 5° [53]. Most of the available experimental and numerical results are limited to a single blade section and, therefore it is difficult to relate these results for an actual wind turbine and use them to evaluate operational strategies.

4. Further work

The energy yield assessment for the chosen strategies was conducted for a 24-hour period of operation with icing events of either 1 or 4 h duration. The viability results for AIS – based on the number of icing days – and derating therefore do not take into account the possibility of multiple icing events occurring in a single day. Seasonal, yearly and event-based analysis can be developed by including various scenarios, which will be especially valuable for the day ahead estimation of energy prices. Future work should focus on the consideration of various scenarios for which a set of operational strategies are implemented and how the performance of the wind turbine can change if the best operational strategy fails. Thus, advanced and complex ice mitigation strategies can be developed to ensure the optimal operation of future wind turbines.

In further work, the sensitivity of the anti-icing viability result should be studied to investigate the impact of the financial assumptions made for electricity price and investment cost in conjunction with anti-icing system layout design and control algorithms. In addition, the viability

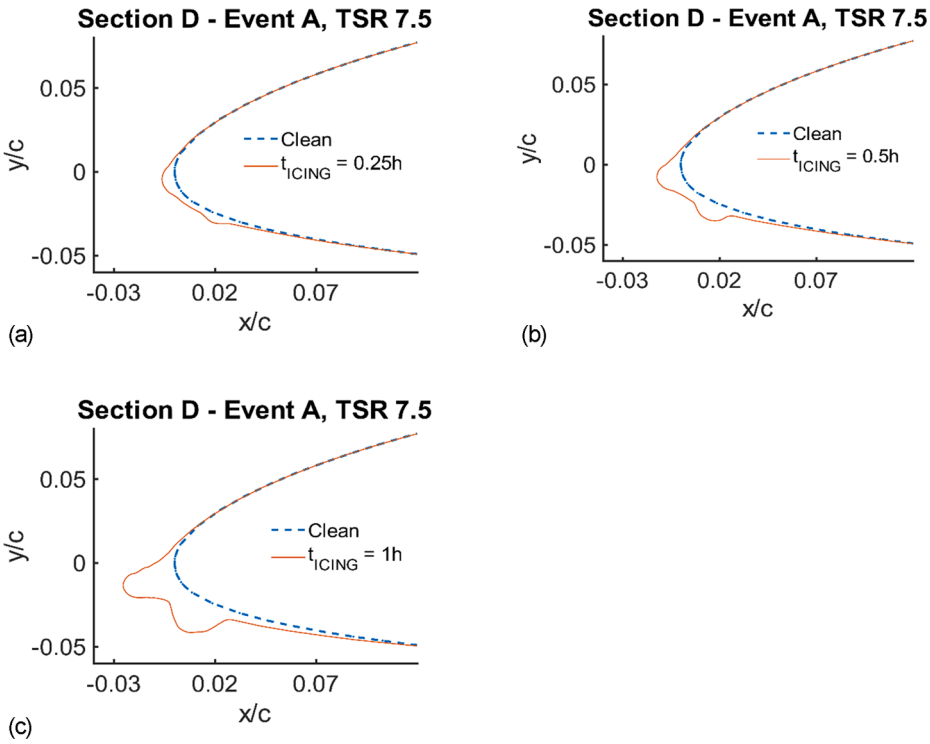

Fig. 12. a-c: Ice shapes generated with LewINT® for the 1-hour icing event at 0.25, 0.5 and 1.0 h, (a), (b), and (c) respectively; and tested in a low speed wind tunnel at a Re of 165 000.

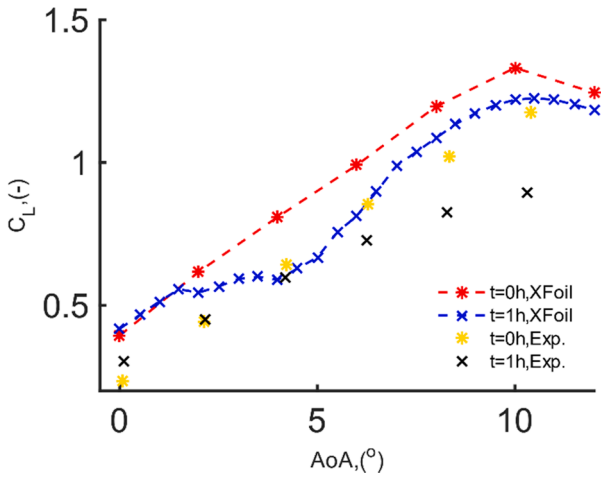

Fig. 13. Experimental and simulation results obtained with XFoil showing the degradation of C_L charactetistics at section D for icing event A.

analysis can be improved by accounting for the efficiency of anti-icing systems as suggested in [45]. The financial viability analysis could also be improved to account for the additional cost of implementing derating. Structural and dynamic analysis, by using the total ice mass, could show that due to fatigue loads the wind turbine structural integrity might need additional reinforcement leading to additional cost for implementation. Blade material damage from different AIS designs and strategies also needs to be carefully evaluated. The method used in this study involved relatively inexpensive aerodynamic computations, but higher fidelity analysis tools can be used in the future following the same approach.

The method presented in this paper can be adopted for evaluating other wind turbines, locations, icing events and operational approaches for ice mitigation; however, this will require:

- Improved ice climate mapping, information on the expected icing intensity and icing event distribution in local regions
- Higher accuracy aerodynamic analysis tools for modelling aerofoils with abrupt shapes on the leading edge; in this study it was found that lift reduction varied between 3.9% and 26% depending on the aerodynamic analysis tool used
- More data on ice mitigation strategy performance over long-term periods and details on cost and maintenance
- Incorporation of dynamic analyses to inform wind turbine operations in real-time, as the current method proposed in this research is limited to event-based modelling

Moreover, the method can be extended to include monthly and yearly net energy losses using statistical data for icing events, such as frequency and intensity distributions. To better define the duration and the impact of the icing events, ice reduction mechanisms should be incorporated in the ice accretion models. This will help evaluate the impact of all operational strategies. To realise the full benefit of combining alternative ice-mitigation operational strategies, a number of advancements will be needed in:

- Sensing equipment to i) monitor icing-event, post-icing and environmental parameters, and ii) detect and characterise ice accretion along the length of turbine blades
- Dynamic control algorithms with artificial intelligence for selecting different operational regimes.
- Prototyping and testing of emerging ice-mitigation strategies in collaboration with operators and manufacturers
- Anti-icing system design to optimise blade surface protection area, accurately control surface temperatures, prevent material damage and reduce installation, operating and maintenance costs.

5. Conclusion

This research found that derating can increase power production in

comparison to anti-icing and reference operating procedures for a utility-scale wind turbine during certain icing conditions. Anti-icing was found to be preferable for short extreme and long mild icing conditions; however, anti-icing system viability is highly sensitivity to the cost of implementation and surface protection area, which will require further advancements to be made in anti-icing system design. Our findings highlight the importance of having a combination of alternative ice mitigation strategies embedded into installed wind turbines in cold climates, and operational procedures in place for strategy selection, where strategy selection considers carefully daily net energy losses, ice mass accumulation, icing event frequency and financial payback times.

CRediT authorship contribution statement

D.B. Stoyanov: Conceptualization, Methodology, Software, Validation, Formal analysis, Investigation, Resources, Data curation, Writing - original draft, Visualization, Project administration. **J.D. Nixon:** Conceptualization, Methodology, Resources, Writing - review & editing, Supervision, Project administration, Funding acquisition. **H. Sarlak:** Conceptualization, Methodology, Writing - review & editing, Supervision, Project administration.

Declaration of Competing Interest

The authors declare that there is no conflict of interest.

References

[1] Bredesen RE, Cattin R, Clausen N, Davis N, Jordaens PJ, Khadri-Yazami Z et al. Wind Energy Projects in Cold Climates; 2017.
[2] Laakso T, Baring-Gould I, Durstewitz M, Horbaty R, Lacroix A, Peltola E et al. State-of-the-art of wind energy in cold climates; 2010.
[3] Tammelin B, Cavaliere M, Holttinen H, Morgan C, Seifret H, Santti K. Wind Energy Production in Cold Climates (WECO); 2000.
[4] Baring-Gould I, Tallhaug L, Vindteknikk K, Ronsten G, Horbaty R, Cattin R et al. Expert Group Study On Recommendations for Wind Energy Projects in Cold Climates; 2010.
[5] Sarlak H, J Sørensen N. Analysis of throw distances of detached objects from horizontal-axis wind turbines. Wind Energy 2015;19. 12/02/2020-151-166.
[6] Fakorede O, Feger Z, Ibrahim H, Ilinca A, Perron J, Masson C. Ice protection systems for wind turbines in cold climate: characteristics, comparison and analysis. Renew Sustain Energy Rev 2016;65:662.
[7] Cattin R. Icing of Wind Turbines. Elforsk. 2012;12(13):23.
[8] Dalili N, Edrisy A, Carriveau R. A review of surface engineering issues critical to wind turbine performance. Renew Sustain Energy Rev 2007;13:428–38.
[9] Parent O, Ilinca A. Anti-icing and de-icing techniques for wind turbines. Crit Rev Cold Regions Sci Technol 2011;65:88–96.
[10] Gao L, Liu Y, Ma L, Hu H. A hybrid strategy combining minimized leading-edge electric-heating and superhydro-/ice-phobic surface coating for wind turbine icing mitigation. Renew Energy 2019;140:943–56.
[11] Madi E, Pope K, Huang W, Iqbal T. A review of integrating ice detection and mitigation for wind turbine blades. Renew Sustain Energy Rev 2019;103:269–81.
[12] Lehtomaki V, Krenn A, Jordaens PJ, Godreau C, Davis N, Khadiri-Yazami Z et al. Available Technologies for Wind Energy in Cold Climates; 2018.
[13] Villalpando F, Reggio M, Ilinca A. Prediction of ice accretion and anti-icing heating power on wind turbine blades using standard commercial software. Energy 2016;114:1041–52.
[14] Reid T, Baruzzi G, Ozcer I, Switchenko D, Habashi WG. FENSAP-ICE Simulation of Icing on Wind Turbine Blades, Part 2: Ice Protection System Design, AIAA2013-0751. (2013) 1.
[15] Mayer C, Ilinca A, Fortin G, Perron J. Wind tunnel study of the elecro-thermal de-icing of wind turbine blades. Int J Offshore Polar Eng 2007;17:3.
[16] Raj LP, Myong RS. Computational analysis of an electro-thermal ice protection system in atmospheric icing conditions. Comput Fluids 2016;21:1.
[17] Fortin G, Perron J. Wind Turbine Icing and De-Icing, American Institute of Aeronautics and Astronautics Journal. (2009) 1-21.
[18] Stoyanov DB, Nixon JD. Alternative operational strategies for wind turbines in cold climates. Renew Energy 2020;145:2694–706.
[19] Zanon A, Gennaro De M, Kuhnelt H. Wind energy harnessing of the NREL 5 MW reference wind turbine in icing conditions under different operational strategies. Renew Energy 2018;115:760–72.
[20] Brillembourg D. Turbines under atmospheric icing conditions - ice accretion modelling, aerodynamics, and control strategies for mitigating performance degradation. Wind Energy 2013;20:601–17.
[21] Laakso T, Peltola E. Review on blade heating technology and future prospects. BOREAS VII Proceedings. 2005.
[22] Barber S, Chokani N, Abhari R. Assessment of wind turbine performance in alpine environments. Wind Eng 2011;35:313–28.
[23] Kolar S. A Comparison of Wind Power Production with Three Different De- and Anti-Icing Systems, UPTEC ES. Independent thesis Advanced level (professional degree) (2015) 58.
[24] K Sachse, Nordex Advanced Anti-Icing System for N149/4.0-4.5, (2020).
[25] Peltola E, Marjaniemi M, Stiesdal H, Jarvela J. An ice prevention system for the wind turbine blades. European Wind Energy Conference 1999:1034.
[26] Roberge P, Lemay J, Ruel J, Bégin-Drolet A. Field analysis, modeling and characterization of wind turbine hot air ice protection systems. Cold Reg. Sci. Technol. 2019;163:19–26.
[27] Cattin R, Kunz S, Heimo A, Russi M, Russi G. Two years of monitoring of a wind turbine under icing conditions; 2008.
[28] Battisti L, Fedrizzi R, Dal Salvio S, Giovannelli A. Influence of the type and size on wind turbines on anti-icing thermal power requirements for blades. EUROMECH Colloquium 464b on Wind Energy 2007.
[29] Homola MC, Virk MS, Nicklasson PJ, Sundsbø PA. Performance losses due to ice accretion for a 5 MW wind turbine. Wind Energ. 2012;15:379–89.
[30] Wright W. User's Manual for LEWICE Version 2008;3:2.
[31] Marten D, Wendler J. Qblade Guidelines 2013.
[32] Etemaddar M, Hansen M, Mo T. Wind turbine aerodynamic response under atmospheric icing conditions. Wind Energy 2012;17:241–65.
[33] Lamraoui F, Fortin G, Benoit R, Perron J, Masson C. Atmospheric icing severity: quantification and mapping. Atmos Res 2013;128:57–75.
[34] Homola M, Wallenius T, Makkonen L, Nicklasson P, Sundsbo P. Turbine size and temperature dependence of icing on wind turbine blades. Wind Eng. 2010;34.
[35] Han Y, Palacios J, Schmitz S. Scaled ice accretion experiments on a rotating wind turbine blade. J Wind Eng Ind Aerodyn 2012;109:55–67.
[36] Hu L, Zhu X, Hu C, Chen J, Du Z. Wind turbine ice distribution and load response under icing condition. Renewable Energy 2017;113:608–19.
[37] COST-727, Atmospheric Icing on Structures, Measurements and Data Collection on Icing: State of the Art, (2006) 14.
[38] Al-Khalil KM, Horvarth C, Miller DR, W Wright B. Validation of NASA Therma Ice Protection Computer Codes, NASA. TM-2001-210907; 1997.
[39] P Suke, Analysis of Heating Systems to Mitigate Ice Accretion on Wind Turbine Blades, (2014).
[40] Makkonen L, Laakso T, Marjaniemi M, Finstad JK. Modelling and prevention of ice accretion on wind turbines. Wind Eng 2001;25. 3-3-21.
[41] L Battisti, Chapter 4 Icing Process, Wind Turbines in Cold Climates, Springer, Switzerland; 2015. p. 177-248.
[42] T Myers G, J Charpin, C Thompson P. Slowly accreting ice due to supercooled water impacting on a cold surface, Physics of Fluids 2002;14:240–256.
[43] Fakorede O, Ibrahim H, Ilinca A, Perron J. Experimental investigation of power requirements for wind turbines electrothermal anti-icing systems. Wind Turbines - Design, Control and Applications; 2016.
[44] Dierer S, Oechslin R, Cattin R. Wind turbines in icing conditions: performance and prediction. Adv Sci Res 2011;6:245–50.
[45] Battisti L. Wind Turbines in Cold Climates. 1st ed. Springer International Publishing; 2015.
[46] IRENA. Renewable Energy technologies: Cost Analysis Series, Wind Power, International Renewable Energy Agency, Abu Dhabi; 2012. p. 19-18-22.
[47] IRENA, Renewable Power Generation Const in 2018, International Renewable Energy Agency, Abu Dhabi. ISBN 978-92-9260-126-3 (2019) 19-18-20.
[48] T Stehly, P Beiter, 2018 Cost of Wind Energy Review, NREL/TP-5000-74598 (2018).
[49] Jonkman J, Butterfield S, Musial W, Scott G. Definition of a 5-MW Reference Wind Turbine of Offshore System Development; 2009.
[50] Hudecz A. Icing Problems of Wind Turbine Blades in Cold Climates, Department of Wind Energy, Technical University of Denmark; 2014.
[51] Dimitrova M, Ibrahim H, Fortin G, Ilinca A, Perron J. Software tool to predict the wind energy production losses due to icing. IEEE Electrical Power Energy Conference 2011:462.
[52] TecQuipment, AFA3 User Guides; 2013.
[53] Han W, Kim J, Kim B. Study on correlation between wind turbine performance and ice accretion along a blade tip airfoil using CFD. J Renewable Sustainable Energy 2018;10:023306.